

Physical Layer Network Coding for FSK Systems

Sørensen, Jesper Hemming; Krigslund, Rasmus; Popovski, Petar; K. Akino, Toshiaki; Larsen, Torben

Published in:
IEEE Communications Letters

DOI (link to publication from Publisher):
[10.1109/LCOMM.2009.090981](https://doi.org/10.1109/LCOMM.2009.090981)

Publication date:
2009

Document Version
Publisher's PDF, also known as Version of record

[Link to publication from Aalborg University](#)

Citation for published version (APA):
Sørensen, J. H., Krigslund, R., Popovski, P., K. Akino, T., & Larsen, T. (2009). Physical Layer Network Coding for FSK Systems. *IEEE Communications Letters*, 13(8), 597-599. <https://doi.org/10.1109/LCOMM.2009.090981>

General rights

Copyright and moral rights for the publications made accessible in the public portal are retained by the authors and/or other copyright owners and it is a condition of accessing publications that users recognise and abide by the legal requirements associated with these rights.

- Users may download and print one copy of any publication from the public portal for the purpose of private study or research.
- You may not further distribute the material or use it for any profit-making activity or commercial gain
- You may freely distribute the URL identifying the publication in the public portal -

Take down policy

If you believe that this document breaches copyright please contact us at vbn@aub.aau.dk providing details, and we will remove access to the work immediately and investigate your claim.

Physical Layer Network Coding for FSK Systems

Jesper H. Sørensen, Rasmus Krigslund, Petar Popovski, Toshiaki Koike Akino, and Torben Larsen

Abstract—In this work we extend the existing concept of De-Noise and Forward (DNF) for bidirectional relaying to utilise non-coherent modulation schemes. This is done in order to avoid the requirement of phase tracking in coherent detection. As an example BFSK is considered, and through analysis the decision regions for the denoise operation in DNF are identified. The throughput performance of BFSK in DNF is compared to BPSK.

Index Terms—Physical layer network coding; frequency shift keying; non-coherent modulation.

I. INTRODUCTION

BIDIRECTIONAL relaying has been the focus of much research within wireless communication recently, [1]–[4]. Traditionally the three node scenario, where nodes A and B communicate with each other through a relaying node R, is considered. Examples of bidirectional relay protocols are Amplify-and-Forward, AF, and Decode-and-Forward, DF, [5], where DF is illustrated in Fig. 1(a). In [6] a concept called DeNoise-and-Forward, DNF, is presented. Here nodes A and B transmit their packets to the relay simultaneously. Assuming proper synchronisation, the signals are added in the air, which is referred to as analog network coding. The relay maps the resulting symbols to a binary message indicating that either equal or different symbols were received. The relay broadcasts this message, which makes an end node able to reconstruct its intended packet by knowing what it transmitted to the relay. Fig. 1(b) shows how packets can be exchanged in only two time slots, when using DNF. The mapping of received symbols to a binary message is effectively a remodulation performed in the physical layer, which removes the noise added during transmissions to the relay. This means that the packets are denoised, although decoding is not performed, hence the name.

In [6] BPSK modulation is applied in DNF, hence it is necessary to assume symbol synchronisation and coherent detection. The phase tracking required for coherent detection is impractical, hence non-coherent modulation schemes should be investigated. In this paper we investigate the use of BFSK modulation in DNF. Optimum decision regions are determined through analysis and the expected throughput is presented and compared to that of BPSK in DF and DNF respectively.

II. ANALYSIS OF DECISION REGIONS FOR BFSK

When analysing the decision regions we assume AWGN channels with no interference from other sources. We account for propagation loss and ergodic phase fading, where the

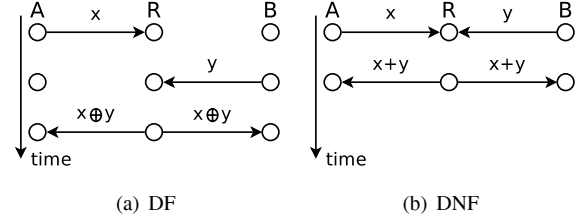


Fig. 1. Existing approaches to bidirectional relaying.

phase, ϕ , is uniformly distributed between 0 and 2π . Moreover, symbol synchronisation in joint transmissions is assumed.

FSK systems rely on envelope detection using quadrature receivers. Hence, the received signal is four dimensional and Gaussian noise components, ω_i , are added to each dimension respectively. The two possible received signals are represented as the following vectors:

$$x_1 = \left(\underbrace{\sqrt{E_s} \cos \phi_1 + \omega_1, \sqrt{E_s} \sin \phi_1 + \omega_2}_{\alpha}, \underbrace{\omega_3, \omega_4}_{\beta} \right) \quad (1)$$

$$x_2 = \left(\omega_1, \omega_2, (\sqrt{E_s} \cos \phi_2 + \omega_3), (\sqrt{E_s} \sin \phi_2 + \omega_4) \right) \quad (2)$$

The envelope in both frequency bands can be calculated from dimensions 1 plus 2 and 3 plus 4, marked by α and β respectively. Note that assuming AWGN, the envelope in a frequency band containing the signal is Rician distributed, while the envelope in a frequency band containing only noise is Rayleigh distributed.

In DNF there exist a significant difference between BPSK and BFSK. For BPSK the transmitted signals are either in phase or in reverse phase, which means that they can be added as scalars. In BFSK, however, they must be added as vectors due to the unknown phase difference. With two possible symbols we have four possible combinations in a joint transmission from nodes A and B. These are denoted x_{ij} where ij refers to the combination of x_1 and x_2 from Eqn. (1) and (2).

$$\begin{aligned} x_{11} &= \left((\sqrt{E_{sA}} \cos \phi_{1A} + \sqrt{E_{sB}} \cos \phi_{1B} + \omega_1), \right. \\ &\quad \left. (\sqrt{E_{sA}} \sin \phi_{1A} + \sqrt{E_{sB}} \sin \phi_{1B} + \omega_2), \omega_3, \omega_4 \right) \\ x_{12} &= \left((\sqrt{E_{sA}} \cos \phi_{1A} + \omega_1), (\sqrt{E_{sA}} \sin \phi_{1A} + \omega_2), \right. \\ &\quad \left. (\sqrt{E_{sB}} \cos \phi_{2B} + \omega_3), (\sqrt{E_{sB}} \sin \phi_{2B} + \omega_4) \right) \\ x_{21} &= \left((\sqrt{E_{sA}} \cos \phi_{1B} + \omega_1), (\sqrt{E_{sA}} \sin \phi_{1B} + \omega_2), \right. \\ &\quad \left. (\sqrt{E_{sB}} \cos \phi_{2A} + \omega_3), (\sqrt{E_{sB}} \sin \phi_{2A} + \omega_4) \right) \\ x_{22} &= \left(\omega_1, \omega_2, (\sqrt{E_{sA}} \cos \phi_{2A} + \sqrt{E_{sB}} \cos \phi_{2B} + \omega_3), \right. \\ &\quad \left. (\sqrt{E_{sA}} \sin \phi_{2A} + \sqrt{E_{sB}} \sin \phi_{2B} + \omega_4) \right) \end{aligned}$$

Manuscript received April 28, 2009. The associate editor coordinating the review of this letter and approving it for publication was H.-H. Chen.

J. H. Sørensen, Rasmus Krigslund, Petar Popovski, and Torben Larsen are with Aalborg University, Department of Electronic Systems (e-mail: {champz, raskri, petarp, tl}@es.aau.dk).

T. K. Akino is with Harvard University, School of Engineering and Applied Sciences (e-mail: koike@seas.harvard.edu).

Digital Object Identifier 10.1109/LCOMM.2009.090981

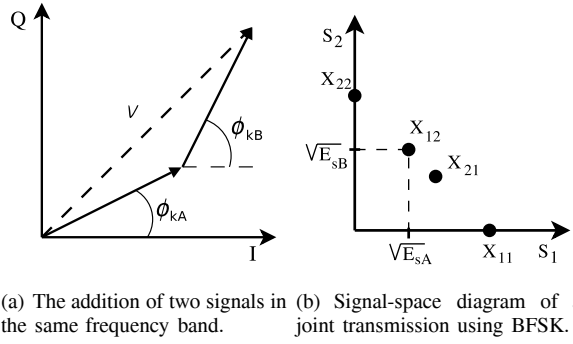


Fig. 2. Existing approaches to bidirectional relaying.

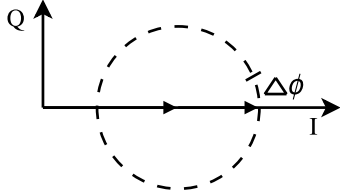


Fig. 3. The possible total signals for uniformly distributed ϕ_d .

The signal components in x_{12} and x_{21} do not interfere, hence the total signal consists of two Rician distributed envelopes. However, when the two nodes transmit the same symbol, the signal components are added. Fig. 2(a) shows a geometrical interpretation of the addition.

The total envelope, ν , detected by the receiver is represented by the dotted line in Fig. 2(a). Depending on the phase difference between the two components, they will either add as scalars, cancel out or something in between. As a result, ν follows a composite distribution, which can be described as a Rician distribution in which the mean value follows some distribution, which is determined later.

Assuming zero phase difference, the envelope of both x_{11} and x_{22} is $\sqrt{E_{sA}} + \sqrt{E_{sB}}$. This is also the coordinate for the symbols in the dimension for the corresponding frequency. The symbols corresponding to x_{12} and x_{21} lie in the first quadrant and if $\sqrt{E_{sA}} = \sqrt{E_{sB}}$ they are represented by the same symbol. If $\sqrt{E_{sA}} \neq \sqrt{E_{sB}}$ however, the symbols are separated resulting in a signal constellation as illustrated in Fig. 2(b), where s_1 and s_2 refers to the dimension of the two frequency bands respectively.

A. Conditional Distributions

The four possible analog coded symbols in BFSK do not follow the same type of distribution, hence the optimum decision regions can not be defined using Maximum Likelihood (ML) detection. Instead Maximum A posteriori Probability (MAP) detection is applied, where the conditional probability density functions of the possible symbols are compared. Note that in DNF we only discriminate between the symbols with equal frequencies and the symbols with different frequencies. Hence the two dimensional space in Fig. 2(b) should be divided into two regions based on the conditional PDFs.

In the case where the received symbol contains different frequencies the total signal is a two dimensional vector, whose elements both follow a Rician distribution. A signal vector is defined by the random variable $U = (U_i, U_j)^T$, where U_i and

U_j are the envelopes in the two frequency bands respectively. Hence, the joint conditional PDF of U is:

$$f_U(U|s_{ij}) = \frac{U_i U_j}{\sigma^4} \exp\left(\frac{-(U_i^2 + E_{sA}) - (U_j^2 + E_{sB})}{2\sigma^2}\right) \cdot I_0\left(\frac{U_i \sqrt{E_{sA}}}{\sigma^2}\right) I_0\left(\frac{U_j \sqrt{E_{sB}}}{\sigma^2}\right) \quad (3)$$

Where s_{ij} is the transmitted symbol, and ij is either 12 or 21. I_0 is the modified zero order Bessel function. Assuming that all symbols are equiprobable, the total joint PDF for symbols with different frequencies is:

$$f_U(U|s_{ij}, i \neq j) = \frac{1}{2}(f_U(U|s_{12}) + f_U(U|s_{21})) \quad (4)$$

When the two transmitters use the same frequency, the remaining frequency band contains only noise. These noise components, ω_i , are orthogonal, hence the resulting envelope is Rayleigh distributed with parameter σ since $\omega_i \sim \mathcal{N}(0, \sigma^2)$. This envelope is referred to as U_k , where $k = 2$ if s_{11} is transmitted and vice versa.

$$f_{U_k}(U_k|s_{ij}, i = j) = \frac{U_k}{\sigma^2} \exp\left(\frac{-U_k^2}{2\sigma^2}\right) \quad (5)$$

The envelope in the used frequency band, U_l , where $l = 1$ if s_{11} is transmitted, follows a composite distribution as stated earlier. This distribution is a Rician distribution where the mean value itself follows a distribution. This composite distribution can be expressed as follows.

$$f_{U_l}(U_l|s_{ij}, i = j) = \int_{-\infty}^{\infty} f_{\nu}(\nu) \cdot \frac{U_l}{\sigma^2} \exp\left(\frac{-(U_l^2 + \nu^2)}{2\sigma^2}\right) I_0\left(\frac{U_l \nu}{\sigma^2}\right) d\nu \quad (6)$$

The mean value is the noiseless envelope, ν , whose distribution is a result of the uniform distribution of the phase difference, $\phi_d = \phi_{kB} - \phi_{kA}$, where k refers to the transmitted frequency. The value of ν depends on ϕ_d and not the individual values of ϕ_{kA} and ϕ_{kB} , hence ϕ_{kA} is used as reference.

In order to derive the distribution of ν , we first consider a probability mass function, PMF. This is a discrete expression of the distribution of ν , i.e. it expresses the probability of experiencing a ν within a certain $\Delta\nu = [\nu_a; \nu_b]$. A certain $\Delta\nu$ corresponds to a certain $\Delta\phi$, whose relationship is expressed by the difference quotient $\frac{\Delta\phi}{\Delta\nu}$. Note that the probability of experiencing a ν within $\Delta\nu$ can be expressed as $\frac{\Delta\phi}{\pi}$, because ϕ is uniformly distributed between 0 and 2π and ν is symmetric around π in this interval, as illustrated in Fig. 3. The PMF can thus be expressed as $\frac{\Delta\phi}{\pi\Delta\nu}$ and for $\Delta\nu \rightarrow 0$ this becomes $\frac{d\phi}{\pi d\nu}$, which expresses the PDF we are looking for. This is derived as follows:

$$\begin{aligned} \nu &= \sqrt{(\sqrt{E_{sA}} + \sqrt{E_{sB}} \cos \phi)^2 + (\sqrt{E_{sB}} \sin \phi)^2} \\ \phi &= \cos^{-1}\left(\frac{\nu^2 - E_{sA} - E_{sB}}{2\sqrt{E_{sA}}\sqrt{E_{sB}}}\right) \\ f_{\nu}(\nu) &= \frac{d\phi}{\pi d\nu} = \frac{-\nu}{\pi\sqrt{E_{sA}}\sqrt{E_{sB}}\sqrt{1 - \left(\frac{\nu^2 - E_{sA} - E_{sB}}{2\sqrt{E_{sA}}\sqrt{E_{sB}}}\right)^2}} \quad (7) \end{aligned}$$

By combining Eq. (5), (6) and (7) the joint conditional PDFs of symbols x_{ij} , when i and j are equal, can be expressed as $f_U(U|s_{ij}) = f_{U_k}(U_k|s_{ij}) \cdot f_{U_l}(U_l|s_{ij})$. Hence the total PDF of symbols with equal frequencies is then as follows:

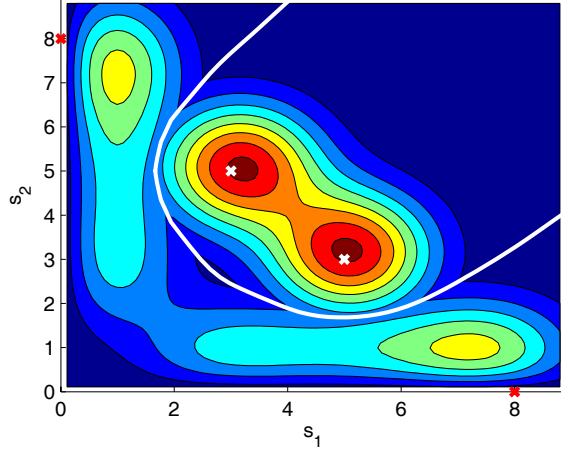


Fig. 4. Both PDFs for $\sqrt{E_{sA}} = 5$, $\sqrt{E_{sB}} = 3$ and $\sigma = 1$.

$$f_U(U|s_{ij}, i = j) = \frac{1}{2}(f_U(U|s_{11}) + f_U(U|s_{22}))$$

B. The Resulting Decision Regions

According to the MAP detection rule, any point in the two dimensional space in Fig. 2(b) should belong to the region represented by the conditional PDF with the highest density in that particular point. This means that the intersection of the two conditional PDFs comprises the bound of the decision region. In Fig. 4 both PDFs are plotted as a contour plot.

The intersection between the two conditional PDFs is found by solving the following equation:

$$f_U(U|s_{ij}, i \neq j) = f_U(U|s_{ij}, i = j) \quad (8)$$

This is a complex equation, hence in this work it has been solved numerically. This has been done by considering a set of fixed envelopes in s_1 and solving the corresponding equations with only the single variable s_2 . A curve indicating the decision region bound can be found by interpolating the solutions. This curve is plotted in Fig. 4 and it agrees with the decision regions indicated by the contour plot.

III. RESULTS

It is known that BPSK outperforms BFSK in regular single link transmissions with respect to BER performance. In this section we compare the performances of the two modulation schemes when applied in DNF and DF respectively.

The BER for BFSK in DNF is determined using a simulation for SNR values between 6 and 23 dB in steps of 1, where $E_{sA} = E_{sB} = 1$. Decision regions for all SNR values are determined as described in section II. As a performance measure we plot the expected throughput, $E[t]$, as a function of SNR, where we assume that the two links have equal SNR ranging from 6 to 23 dB and packets have a length of 128 bytes. In Fig. 5 the expected throughput using DNF and DF is plotted for each modulation scheme respectively. The performance of BPSK in DNF is determined through the analysis in [7]. The results show that using BFSK requires a higher SNR before the throughput converges to its maximal value. DF with BFSK requires ~ 4 dB higher SNR, where DNF with BFSK an increase of ~ 6 dB. In this way the penalty for using BFSK is more significant in DNF. However, the

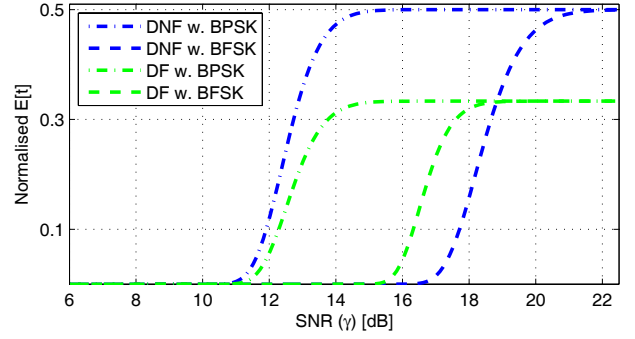


Fig. 5. The expected throughput for DNF and DF using BPSK and BFSK respectively.

denoise operation saves a time slot compared to DF, hence the DNF scheme converges to a throughput of 0.5 compared to the 0.33 for DF. If fading was taken into account the relative performance of DNF and DF would be similar, however, a larger SNR would be required before converging to maximum throughput. This is the case for both modulation schemes.

IV. CONCLUSION

The existing concept of De-Noise and Forward (DNF) is based on the coherent modulation scheme BPSK, where the required tracking of phase is impractical. Therefore, this work have extended the concept of DNF to utilise non-coherent modulation schemes, where we have considered BFSK. The decision regions have been identified through analysis. Results shows that BFSK in DNF yields a lower performance compared to BPSK in DNF, as it requires a higher SNR before communication is possible. Hence being independent of the phase requires a larger SNR in order to obtain the same throughput as for BPSK.

ACKNOWLEDGEMENT

This work has partially been supported by the Danish Research Council for Technology and Production.

REFERENCES

- [1] P. Popovski and H. Yomo, "Bi-directional amplification of throughput in a wireless multi-hop network," in *Proc. 2006 IEEE 63rd Vehicular Technology Conference*, vol. 2, Melbourne, Australia, p. 588, May 2006.
- [2] S. Katti, H. Rahul, W. Hu, D. Katabi, M. Médard, and J. Crowcroft, "XORs in the air: practical wireless network coding," *IEEE Trans. Networking*, vol. 16, no. 3, pp. 497–510, 2008.
- [3] T. J. Oechtering and H. Boche, "Relay selection in bidirectional relay communication," in *Proc. 2007 IEEE 8th Workshop on Signal Processing Advances in Wireless Communications*, Helsinki, Finland, p. 5, June 2007.
- [4] S. Zhang, S. C. Liew, and P. P. Lam, "Hot topic: physical-layer network coding," in *Proc. 12th Annual International Conference on Mobile Computing and Networking (MobiCom'06)*, pp. 358–365, Sept. 2006.
- [5] S. J. Kim, N. Devroye, P. Mitran, and V. Tarokh, "Comparison of bi-directional relaying protocols," in *Proc. 2008 IEEE Sarnoff Symposium*, Princeton, NJ, USA, p. 1, Apr. 2008.
- [6] P. Popovski and H. Yomo, "The anti-packets can increase the achievable throughput of a wireless multi-hop network," in *Proc. 2006 IEEE International Conference on Communications*, vol. 9, Istanbul, Turkey, p. 3885, June 2006.
- [7] J. H. Sørensen, R. Krigslund, P. Popovski, T. K. Akino, and T. Larsen, "Scalable denoise-and-forward in bidirectional relay networks," *Computer Networks (submitted)*, 2009. Available from: <http://kom.aau.dk/group/09gr1010/ScalableDNFelsevier.pdf>.